Comparison of Non-Intrusive Polynomial Chaos and Stochastic Collocation Methods for Uncertainty Quantification

M. S. Eldred*
Sandia National Laboratories†, Albuquerque, NM 87185

J. Burkardt‡
Virginia Tech, Blacksburg, VA 24061

Non-intrusive polynomial chaos expansion (PCE) and stochastic collocation (SC) methods are attractive techniques for uncertainty quantification (UQ) due to their strong mathematical basis and ability to produce functional representations of stochastic variability. PCE estimates coefficients for known orthogonal polynomial basis functions based on a set of response function evaluations, using sampling, linear regression, tensor-product quadrature, or Smolyak sparse grid approaches. SC, on the other hand, forms interpolation functions for known coefficients, and requires the use of structured collocation point sets derived from tensor-products or sparse grids. When tailoring the basis functions or interpolation grids to match the forms of the input uncertainties, exponential convergence rates can be achieved with both techniques for general probabilistic analysis problems. In this paper, we explore relative performance of these methods using a number of simple algebraic test problems, and analyze observed differences. In these computational experiments, performance of PCE and SC is shown to be very similar, although when differences are evident, SC is the consistent winner over traditional PCE formulations. This stems from the practical difficulty of optimally synchronizing the form of the PCE with the integration approach being employed, resulting in slight over- or under-integration of prescribed expansion form. With additional nontraditional tailoring of PCE form, it is shown that this performance gap can be reduced, and in some cases, eliminated.

I. Introduction

Uncertainty quantification (UQ) is the process of determining the effect of input uncertainties on response metrics of interest. These input uncertainties may be characterized as either aleatory uncertainties, which are irreducible variabilities inherent in nature, or epistemic uncertainties, which are reducible uncertainties resulting from a lack of knowledge. Since sufficient data is generally available for aleatory uncertainties, probabilistic methods are commonly used for computing response distribution statistics based on input probability distribution specifications. Conversely, for epistemic uncertainties, data is generally sparse, making the use of probability distribution assertions questionable and typically leading to nonprobabilistic methods based on interval specifications.

One technique for the analysis of aleatory uncertainties using probabilistic methods is the polynomial chaos expansion (PCE) approach to UQ. In this work, we focus on generalized polynomial chaos using the Wiener-Askey scheme,[1] in which Hermite, Legendre, Laguerre, Jacobi, and generalized Laguerre orthogonal polynomials are used for modeling the effect of uncertain variables described by normal, uniform, exponential,

*Principal Member of Technical Staff, Optimization and Uncertainty Estimation Department, MS-1318, Associate Fellow AIAA.

†Sandia is a multiprogram laboratory operated by Sandia Corporation, a Lockheed Martin Company, for the United States Department of Energy's National Nuclear Security Administration under Contract DE-AC04-94AL85000.

‡Computational Science Specialist, Advanced Research Computation group.

beta, and gamma probability distributions, respectively[a]. These orthogonal polynomial selections are optimal for these distribution types since the inner product weighting function and its corresponding support range correspond to the probability density functions for these continuous distributions. In theory, exponential convergence rates can be obtained with the optimal basis. When transformations to independent standard random variables (in some cases, approximated by uncorrelated standard random variables) are used, the variable expansions are uncoupled, allowing the polynomial orthogonality properties to be applied on a per-dimension basis. This allows one to mix and match the polynomial basis used for each variable without interference with the spectral projection scheme for the response.

In non-intrusive PCE, simulations are used as black boxes and the calculation of chaos expansion coefficients for response metrics of interest is based on a set of simulation response evaluations. To calculate these response PCE coefficients, two primary classes of approaches have been proposed: spectral projection and linear regression. The spectral projection approach projects the response against each basis function using inner products and employs the polynomial orthogonality properties to extract each coefficient. Each inner product involves a multidimensional integral over the support range of the weighting function, which can be evaluated numerically using sampling, quadrature, or sparse grid approaches. The linear regression approach (also known as point collocation or stochastic response surfaces) uses a single linear least squares solution to solve for the PCE coefficients which best match a set of response values obtained from a design of computer experiments.

Stochastic collocation (SC) is another stochastic expansion technique for UQ that is closely related to PCE. Whereas PCE estimates coefficients for known orthogonal polynomial basis functions, SC forms Lagrange interpolation functions for known coefficients. Since the i^{th} interpolation function is 1 at collocation point i and 0 for all other collocation points, it is easy to see that the expansion coefficients are just the response values at each of the collocation points. The formation of multidimensional interpolants with this property requires the use of structured collocation point sets derived from tensor products or sparse grids. The key to the approach is performing collocation using the Gauss points and weights from the same optimal orthogonal polynomials used in generalized PCE, which results in the same exponential convergence rates. A key distinction is that, whereas PCE must define an expansion formulation and a corresponding coefficient estimation approach (which may not be perfectly synchronized), SC requires only a collocation grid definition from which the expansion polynomials are derived based on Lagrange interpolation.

Section II describes the orthogonal polynomial and interpolation polynomial basis functions, Section III describes the generalized polynomial chaos and stochastic collocation methods in additional detail, Section IV describes non-intrusive approaches for calculating the polynomial chaos coefficients or forming the set of stochastic collocation points, Section V presents computational results for a number of benchmark test problems, and Section VI provides concluding remarks.

II. Polynomial Basis

A. Orthogonal polynomials in the Askey scheme

Table 1 shows the set of polynomials which provide an optimal basis for different continuous probability distribution types. It is derived from the family of hypergeometric orthogonal polynomials known as the Askey scheme,[2] for which the Hermite polynomials originally employed by Wiener[3] are a subset. The optimality of these basis selections derives from their orthogonality with respect to weighting functions that correspond to the probability density functions (PDFs) of the continuous distributions when placed in a standard form. The density and weighting functions differ by a constant factor due to the requirement that the integral of the PDF over the support range is one.

Note that Legendre is a special case of Jacobi for $\alpha = \beta = 0$, Laguerre is a special case of generalized Laguerre for $\alpha = 0$, $\Gamma(a)$ is the Gamma function which extends the factorial function to continuous values, and $B(a, b)$ is the Beta function defined as $B(a, b) = \frac{\Gamma(a)\Gamma(b)}{\Gamma(a+b)}$. Some care is necessary when specifying the α and β parameters for the Jacobi and generalized Laguerre polynomials since the orthogonal polynomial conventions[4] differ from the common statistical PDF conventions. The former conventions are used in Table 1.

[a]Orthogonal polynomial selections also exist for discrete probability distributions, but are not explored here.

Table 1. Linkage between standard forms of continuous probability distributions and Askey scheme of continuous hyper-geometric polynomials.

Distribution	Density function	Polynomial	Weight function	Support range
Normal	$\frac{1}{\sqrt{2\pi}} e^{\frac{-x^2}{2}}$	Hermite $He_n(x)$	$e^{\frac{-x^2}{2}}$	$[-\infty, \infty]$
Uniform	$\frac{1}{2}$	Legendre $P_n(x)$	1	$[-1, 1]$
Beta	$\frac{(1-x)^\alpha (1+x)^\beta}{2^{\alpha+\beta+1} B(\alpha+1, \beta+1)}$	Jacobi $P_n^{(\alpha,\beta)}(x)$	$(1-x)^\alpha (1+x)^\beta$	$[-1, 1]$
Exponential	e^{-x}	Laguerre $L_n(x)$	e^{-x}	$[0, \infty]$
Gamma	$\frac{x^\alpha e^{-x}}{\Gamma(\alpha+1)}$	Generalized Laguerre $L_n^{(\alpha)}(x)$	$x^\alpha e^{-x}$	$[0, \infty]$

B. Numerically generated orthogonal polynomials

If all random inputs can be described using independent normal, uniform, exponential, beta, and gamma distributions, then generalized PCE can be directly applied. If correlation or other distribution types are present, then additional techniques are required. One solution is to employ nonlinear variable transformations as described in Section III.C such that an Askey basis can be applied in the transformed space. This can be effective as shown in Ref. 5, but convergence rates are typically degraded. In addition, correlation coefficients are warped by the nonlinear transformation,[6] and transformed correlation values are not always readily available. An alternative is to numerically generate the orthogonal polynomials, along with their Gauss points and weights, that are optimal for given random variable sets having arbitrary probability density functions.[7,8] This not only preserves exponential convergence rates, it also eliminates the need to calculate correlation warping. This topic is explored in Ref. 9.

C. Interpolation polynomials

Lagrange polynomials interpolate a set of points in a single dimension using the functional form

$$L_j = \prod_{\substack{k=1 \\ k \neq j}}^{m} \frac{\xi - \xi_k}{\xi_j - \xi_k} \tag{1}$$

where it is evident that L_j is 1 at $\xi = \xi_j$, is 0 for each of the points $\xi = \xi_k$, and has order $m - 1$.

For interpolation of a response function R in one dimension over m points, the expression

$$R(\xi) \cong \sum_{j=1}^{m} r(\xi_j)\, L_j(\xi) \tag{2}$$

reproduces the response values $r(\xi_j)$ at the interpolation points and smoothly interpolates between these values at other points. For interpolation in multiple dimensions, a tensor-product approach is used wherein

$$R(\boldsymbol{\xi}) \cong \sum_{j_1=1}^{m_{i_1}} \cdots \sum_{j_n=1}^{m_{i_n}} r\left(\xi_{j_1}^{i_1}, \ldots, \xi_{j_n}^{i_n}\right) \left(L_{j_1}^{i_1} \otimes \cdots \otimes L_{j_n}^{i_n}\right) = \sum_{j=1}^{N_p} r_j(\boldsymbol{\xi}) \boldsymbol{L}_j(\boldsymbol{\xi}) \tag{3}$$

where $\boldsymbol{i} = (m_1, m_2, \cdots, m_n)$ are the number of nodes used in the n-dimensional interpolation and $\xi_{j_l}^{i_k}$ is the j_l-th point in the k-th direction. As will be seen later (Section IV.A.3), interpolation on sparse grids involves a summation of these tensor products with varying $\boldsymbol{i}$ levels.

III. Stochastic Expansion Methods

A. Generalized Polynomial Chaos

The set of polynomials from Section II.A are used as an orthogonal basis to approximate the functional form between the stochastic response output and each of its random inputs. The chaos expansion for a response

R takes the form

$$R = a_0 B_0 + \sum_{i_1=1}^{\infty} a_{i_1} B_1(\xi_{i_1}) + \sum_{i_1=1}^{\infty} \sum_{i_2=1}^{i_1} a_{i_1 i_2} B_2(\xi_{i_1}, \xi_{i_2}) + \sum_{i_1=1}^{\infty} \sum_{i_2=1}^{i_1} \sum_{i_3=1}^{i_2} a_{i_1 i_2 i_3} B_3(\xi_{i_1}, \xi_{i_2}, \xi_{i_3}) + ... \quad (4)$$

where the random vector dimension is unbounded and each additional set of nested summations indicates an additional order of polynomials in the expansion. This expression can be simplified by replacing the order-based indexing with a term-based indexing

$$R = \sum_{j=0}^{\infty} \alpha_j \Psi_j(\boldsymbol{\xi}) \quad (5)$$

where there is a one-to-one correspondence between $a_{i_1 i_2 ... i_n}$ and α_j and between $B_n(\xi_{i_1}, \xi_{i_2}, ..., \xi_{i_n})$ and $\Psi_j(\boldsymbol{\xi})$. Each of the $\Psi_j(\boldsymbol{\xi})$ are multivariate polynomials which involve products of the one-dimensional polynomials. For example, a multivariate Hermite polynomial $B(\boldsymbol{\xi})$ of order n is defined from

$$B_n(\xi_{i_1}, ..., \xi_{i_n}) = e^{\frac{1}{2}\boldsymbol{\xi}^T \boldsymbol{\xi}} (-1)^n \frac{\partial^n}{\partial \xi_{i_1} ... \partial \xi_{i_n}} e^{-\frac{1}{2}\boldsymbol{\xi}^T \boldsymbol{\xi}} \quad (6)$$

which can be shown to be a product of one-dimensional Hermite polynomials involving a multi-index m_i^j:

$$B_n(\xi_{i_1}, ..., \xi_{i_n}) = \Psi_j(\boldsymbol{\xi}) = \prod_{i=1}^{n} \psi_{m_i^j}(\xi_i) \quad (7)$$

The first few multidimensional Hermite polynomials for a two-dimensional case (covering zeroth, first, and second order terms) are then

$$\begin{aligned}
\Psi_0(\boldsymbol{\xi}) &= \psi_0(\xi_1)\ \psi_0(\xi_2) &&= 1 \\
\Psi_1(\boldsymbol{\xi}) &= \psi_1(\xi_1)\ \psi_0(\xi_2) &&= \xi_1 \\
\Psi_2(\boldsymbol{\xi}) &= \psi_0(\xi_1)\ \psi_1(\xi_2) &&= \xi_2 \\
\Psi_3(\boldsymbol{\xi}) &= \psi_2(\xi_1)\ \psi_0(\xi_2) &&= \xi_1^2 - 1 \\
\Psi_4(\boldsymbol{\xi}) &= \psi_1(\xi_1)\ \psi_1(\xi_2) &&= \xi_1 \xi_2 \\
\Psi_5(\boldsymbol{\xi}) &= \psi_0(\xi_1)\ \psi_2(\xi_2) &&= \xi_2^2 - 1
\end{aligned}$$

1. Expansion truncation and tailoring

In practice, one truncates the infinite expansion at a finite number of random variables and a finite expansion order

$$R \cong \sum_{j=0}^{P} \alpha_j \Psi_j(\boldsymbol{\xi}) \quad (8)$$

Traditionally, the polynomial chaos expansion includes a complete basis of polynomials up to a fixed total-order specification, in which case the total number of terms N_t in an expansion of total order p involving n random variables is given by

$$N_t = 1 + P = 1 + \sum_{s=1}^{p} \frac{1}{s!} \prod_{r=0}^{s-1} (n + r) = \frac{(n+p)!}{n!p!} \quad (9)$$

This traditional approach will be referred to as a "total-order expansion."

An important alternative approach is to employ a "tensor-product expansion," in which polynomial order bounds are applied on a per-dimension basis (no total-order bound is enforced) and all combinations of the one-dimensional polynomials are included. In this case, the total number of terms N_t is

$$N_t = 1 + P = \prod_{i=1}^{n} (p_i + 1) \quad (10)$$

where p_i is the polynomial order bound for the i-th dimension.

It is apparent from Eq. 10 that the tensor-product expansion readily supports anisotropy in polynomial order for each dimension, since the polynomial order bounds for each dimension can be specified independently. It is also feasible to support anisotropy with total-order expansions, although this involves pruning polynomials that satisfy the total-order bound (potentially defined from the maximum of the per-dimension bounds) but which violate individual per-dimension bounds. In this case, Eq. 9 does not apply.

Additional expansion form alternatives can also be considered. Of particular interest is the tailoring of expansion form to target specific monomial coverage as motivated by the integration process employed for evaluating chaos coefficients. If the specific monomial set that can be resolved by a particular integration approach is known or can be approximated, then the chaos expansion can be tailored to synchonize with this set. Tensor-product and total-order expansions can be seen as special cases of this general approach (corresponding to tensor-product quadrature and Smolyak sparse grids with linear growth rules, respectively), whereas, for example, Smolyak sparse grids with nonlinear growth rules could generate synchonized expansion forms that are neither tensor-product nor total-order (to be discussed later in association with Figure 3). In all cases, the specifics of the expansion are codified in the multi-index, and subsequent machinery for estimating response values at particular $\boldsymbol{\xi}$, evaluating response statistics by integrating over $\boldsymbol{\xi}$, etc., can be performed in a manner that is agnostic to the exact expansion formulation.

2. Dimension independence

A generalized polynomial basis is generated by selecting the univariate basis that is most optimal for each random input and then applying the products as defined by the multi-index to define a mixed set of multivariate polynomials. Similarly, multivariate weighting functions involve a product of the one-dimensional weighting functions and multivariate quadrature rules involve tensor products of the one-dimensional quadrature rules.

The use of independent standard random variables is the critical component that allows decoupling of the multidimensional integrals in a mixed basis expansion. It is assumed in this work that the uncorrelated standard random variables resulting from the transformation described in Section III.C can be treated as independent. This assumption is valid for uncorrelated standard normal variables (and motivates the approach of using a strictly Hermite basis), but may be an approximation for uncorrelated standard uniform, exponential, beta, and gamma variables. For independent variables, the multidimensional integrals involved in the inner products of multivariate polynomials decouple to a product of one-dimensional integrals involving only the particular polynomial basis and corresponding weight function selected for each random dimension. The multidimensional inner products are nonzero only if each of the one-dimensional inner products is nonzero, which preserves the desired multivariate orthogonality properties for the case of a mixed basis.

B. Stochastic Collocation

The SC expansion is formed as a sum of a set of multidimensional Lagrange interpolation polynomials, one polynomial per collocation point. Since these polynomials have the feature of being equal to 1 at their particular collocation point and 0 at all other points, the coefficients of the expansion are just the response values at each of the collocation points. This can be written as:

$$R \cong \sum_{j=1}^{N_p} r_j \boldsymbol{L}_j(\boldsymbol{\xi}) \tag{11}$$

where the set of N_p collocation points involves a structured multidimensional grid. There is no need for tailoring of the expansion form as there is for PCE (see Section III.A.1) since the polynomials that appear in the expansion are determined by the Lagrange construction (Eq. 1). That is, any tailoring or refinement of the expansion occurs through the selection of points in the interpolation grid and the polynomial orders of the basis adapt automatically.

As mentioned in Section I, the key to maximizing performance with this approach is to use the same Gauss points defined from the optimal orthogonal polynomials as the collocation points (using either a tensor product grid as shown in Eq. 3 or a sum of tensor products defined for a sparse grid as shown later in Section IV.A.3). Given the observation that Gauss points of an orthogonal polynomial are its roots, one

can factor a one-dimensional orthogonal polynomial of order p as follows:

$$\psi_j = c_j \prod_{k=1}^{p} (\xi - \xi_k) \tag{12}$$

where ξ_k represent the roots. This factorization is very similar to Lagrange interpolation using Gauss points as shown in Eq. 1. However, to obtain a Lagrange interpolant of order p from Eq. 1 for each of the collocation points, one must use the roots of a polynomial that is one order higher (order $p+1$) and then exclude the Gauss point being interpolated. As discussed later in Section IV.A.2, one also uses these higher order $p+1$ roots to evaluate the PCE coefficient integrals for expansions of order p. Thus, the collocation points used for integration or interpolation for expansions of order p are the same; however, the polynomial bases for PCE (scaled polynomial product involving all p roots of order p) and SC (scaled polynomial product involving p root subset of order $p+1$) are closely related but not identical.

C. Transformations to uncorrelated standard variables

Polynomial chaos and stochastic collocation are expanded using polynomials that are functions of independent standard random variables $\boldsymbol{\xi}$. Thus, a key component of either approach is performing a transformation of variables from the original random variables $\boldsymbol{x}$ to independent standard random variables $\boldsymbol{\xi}$ and then applying the stochastic expansion in the transformed space. The dimension of $\boldsymbol{\xi}$ is typically chosen to correspond to the dimension of $\boldsymbol{x}$, although this is not required. In fact, the dimension of $\boldsymbol{\xi}$ should be chosen to represent the number of distinct sources of randomness in a particular problem, and if individual x_i mask multiple random inputs, then the dimension of $\boldsymbol{\xi}$ can be expanded to accommodate.[10] For simplicity, all subsequent discussion will assume a one-to-one correspondence between $\boldsymbol{\xi}$ and $\boldsymbol{x}$.

This notion of independent standard space is extended over the notion of "u-space" used in reliability methods[11,12] in that in includes not just independent standard normals, but also independent standardized uniforms, exponentials, betas and gammas. For problems directly involving independent normal, uniform, exponential, beta, and gamma distributions for input random variables, conversion to standard form involves a simple linear scaling transformation (to the form of the density functions in Table 1) and then the corresponding chaos/collocation points can be employed. For correlated normal, uniform, exponential, beta, and gamma distributions, the same linear scaling transformation is applied followed by application of the inverse Cholesky factor of the correlation matrix (similar to Eq. 14 below, but the correlation matrix requires no modification for linear transformations). As described previously, the subsequent independence assumption is valid for uncorrelated standard normals but may introduce error for uncorrelated standard uniform, exponential, beta, and gamma variables. For other distributions with a close relationship to variables supported in the Askey scheme (i.e., lognormal, loguniform, and triangular distributions), a nonlinear transformation is employed to transform to the corresponding Askey distributions (i.e., normal, uniform, and uniform distributions, respectively) and the corresponding chaos polynomials/collocation points are employed. For other less directly-related distributions (e.g., extreme value distributions), the nonlinear Nataf transformation is employed to transform to uncorrelated standard normals as described below and Hermite polynomials are employed.

The transformation from correlated non-normal distributions to uncorrelated standard normal distributions is denoted as $\boldsymbol{\xi} = T(\mathbf{x})$ with the reverse transformation denoted as $\mathbf{x} = T^{-1}(\boldsymbol{\xi})$. These transformations are nonlinear in general, and possible approaches include the Rosenblatt,[13] Nataf,[6] and Box-Cox[14] transformations. The nonlinear transformations may also be linearized, and common approaches for this include the Rackwitz-Fiessler[15] two-parameter equivalent normal and the Chen-Lind[16] and Wu-Wirsching[17] three-parameter equivalent normals. The results in this paper employ the Nataf nonlinear transformation, which is suitable for the common case when marginal distributions and a correlation matrix are provided, but full joint distributions are not known[b]. The Nataf transformation occurs in the following two steps. To transform between the original correlated x-space variables and correlated standard normals ("z-space"), a CDF matching condition is applied for each of the marginal distributions:

$$\Phi(z_i) = F(x_i) \tag{13}$$

where $\Phi()$ is the standard normal cumulative distribution function and $F()$ is the cumulative distribution function of the original probability distribution. Then, to transform between correlated z-space variables

[b] If joint distributions are known, then the Rosenblatt transformation is preferred.

and uncorrelated ξ-space variables, the Cholesky factor $\mathbf{L}$ of a modified correlation matrix is used:

$$\mathbf{z} = \mathbf{L}\boldsymbol{\xi} \tag{14}$$

where the original correlation matrix for non-normals in x-space has been modified to represent the corresponding "warped" correlation in z-space.[6]

IV. Non-intrusive methods for expansion formation

The major practical difference between PCE and SC is that, in PCE, one must estimate the coefficients for known basis functions, whereas in SC, one must form the interpolants for known coefficients. PCE estimates its coefficients using any of the approaches to follow: random sampling, tensor-product quadrature, Smolyak sparse grids, or linear regression. In SC, the multidimensional interpolants need to be formed over structured data sets, such as point sets from quadrature or sparse grids; approaches based on random sampling may not be used.

A. Spectral projection

The spectral projection approach projects the response against each basis function using inner products and employs the polynomial orthogonality properties to extract each coefficient. Similar to a Galerkin projection, the residual error from the approximation is rendered orthogonal to the selected basis. From Eq. 8, it is evident that

$$\alpha_j \;=\; \frac{\langle R, \Psi_j \rangle}{\langle \Psi_j^2 \rangle} \;=\; \frac{1}{\langle \Psi_j^2 \rangle} \int_\Omega R\, \Psi_j\, \varrho(\boldsymbol{\xi})\, d\boldsymbol{\xi}, \tag{15}$$

where each inner product involves a multidimensional integral over the support range of the weighting function. In particular, $\Omega = \Omega_1 \otimes \cdots \otimes \Omega_n$, with possibly unbounded intervals $\Omega_j \subset \mathbb{R}$ and the tensor product form $\varrho(\boldsymbol{\xi}) = \prod_{i=1}^{n} \varrho_i(\xi_i)$ of the joint probability density (weight) function. The denominator in Eq. 15 is the norm squared of the multivariate orthogonal polynomial, which can be computed analytically using the product of univariate norms squared

$$\langle \Psi_j^2 \rangle \;=\; \prod_{i=1}^{n} \langle \psi_{m_i^j}^2 \rangle \tag{16}$$

where the univariate inner products have simple closed form expressions for each polynomial in the Askey scheme.[4] Thus, the primary computational effort resides in evaluating the numerator, which is evaluated numerically using sampling, quadrature or sparse grid approaches (and this numerical approximation leads to use of the term "pseudo-spectral" by some investigators).

1. Sampling

In the sampling approach, the integral evaluation is equivalent to computing the expectation (mean) of the response-basis function product (the numerator in Eq. 15) for each term in the expansion when sampling within the density of the weighting function. This approach is only valid for PCE and since sampling does not provide any particular monomial coverage guarantee, it is common to combine this coefficient estimation approach with a total-order chaos expansion.

In computational practice, coefficient estimations based on sampling benefit from first estimating the response mean (the first PCE coefficient) and then removing the mean from the expectation evaluations for all subsequent coefficients.[10] While this has no effect for quadrature/sparse grid methods (see following two sections) and little effect for fully-resolved sampling, it does have a small but noticeable beneficial effect for under-resolved sampling.

2. Tensor product quadrature

In quadrature-based approaches, the simplest general technique for approximating multidimensional integrals, as in Eq. 15, is to employ a tensor product of one-dimensional quadrature rules. In the case where Ω is a hypercube, i.e. $\Omega = [-1, 1]^n$, there are several choices of nested abscissas, included Clenshaw-Curtis,

Gauss-Patterson, etc.[18–20] However, in the tensor-product case, we choose Gaussian abscissas, i.e. the zeros of polynomials that are orthogonal with respect to a density function weighting, e.g. Gauss-Hermite, Gauss-Legendre, Gauss-Laguerre, generalized Gauss-Laguerre, and Gauss-Jacobi.

We first introduce an index $i \in \mathbb{N}_+$, $i \geq 1$. Then, for each value of i, let $\{\xi_1^i, \ldots, \xi_{m_i}^i\} \subset \Omega_i$ be a sequence of abscissas for quadrature on Ω_i. For $f \in C^0(\Omega_i)$ and $n = 1$ we introduce a sequence of one-dimensional quadrature operators

$$\mathscr{U}^i(f)(\xi) = \sum_{j=1}^{m_i} f(\xi_j^i)\, w_j^i, \tag{17}$$

with $m_i \in \mathbb{N}$ given. When utilizing Gaussian quadrature, Eq. 17 integrates exactly all polynomials of degree less than or equal to $2m_i - 1$, for each $i = 1, \ldots, n$. Given an expansion order p, the highest order coefficient evaluations (Eq. 15) can be assumed to involve integrands of at least polynomial order $2p$ (Ψ of order p and R modeled to order p) in each dimension such that a minimal Gaussian quadrature order of $p + 1$ will be required to obtain good accuracy in these coefficients.

Now, in the multivariate case $n > 1$, for each $f \in C^0(\Omega)$ and the multi-index $\mathbf{i} = (i_1, \ldots, i_n) \in \mathbb{N}_+^n$ we define the full tensor product quadrature formulas

$$\mathcal{Q}_{\mathbf{i}}^n f(\xi) = \left(\mathscr{U}^{i_1} \otimes \cdots \otimes \mathscr{U}^{i_n}\right)(f)(\boldsymbol{\xi}) = \sum_{j_1=1}^{m_{i_1}} \cdots \sum_{j_n=1}^{m_{i_n}} f\left(\xi_{j_1}^{i_1}, \ldots, \xi_{j_n}^{i_n}\right) \left(w_{j_1}^{i_1} \otimes \cdots \otimes w_{j_n}^{i_n}\right). \tag{18}$$

Clearly, the above product needs $\prod_{j=1}^n m_{i_j}$ function evaluations. Therefore, when the number of input random variables is small, full tensor-product quadrature is a very effective numerical tool. On the other hand, approximations based on tensor-product grids suffer from the *curse of dimensionality* since the number of collocation points in a tensor grid grows exponentially fast in the number of input random variables. For example, if Eq. 18 employs the same order for all random dimensions, $m_{i_j} = m$, then Eq. 18 requires m^n function evaluations.

Figure 1 displays the monomial coverage for an integrand evaluated using an isotropic Gaussian quadrature rules in two dimensions ($m_1 = m_2 = 5$). Given this type of coverage, the traditional approach of exploying a total-order chaos expansion (involving integrands indicated by the red horizontal line) neglects a significant portion of the monomial coverage and one would expect a tensor-product expansion to provide improved synchronization and more effective usage of the Gauss point evaluations. Note that the integrand monomial coverage must resolve $2p$, such that $p_1 = p_2 = 4$ would be selected in this case.

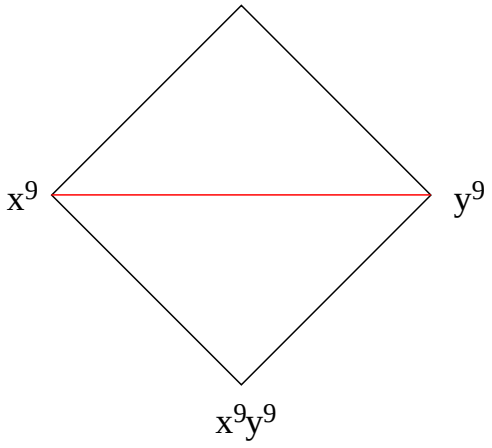

Figure 1. Pascal's triangle depiction of integrand monomial coverage for two dimensions and Gaussian tensor-product quadrature order = 5. Red line depicts maximal total-order integrand coverage.

3. Smolyak sparse grids

If the number of random variables is moderately large, one should rather consider sparse tensor product spaces as first proposed by Smolyak[21] and further investigated by Refs. 18–20, 22–24 that reduce dramatically the number of collocation points, while preserving a high level of accuracy.

Here we follow the notation and extend the description in Ref. 18 to describe the Smolyak *isotropic* formulas $\mathscr{A}(\mathrm{w}, n)$, where w is a level that is independent of dimension[c]. The Smolyak formulas are just linear combinations of the product formulas in Eq. 18 with the following key property: only products with a relatively small number of points are used. With $\mathscr{U}^0 = 0$ and for $i \geq 1$ define

$$\Delta^i = \mathscr{U}^i - \mathscr{U}^{i-1}. \tag{19}$$

and we set $|\mathbf{i}| = i_1 + \cdots + i_n$. Then the isotropic Smolyak quadrature formula is given by

$$\mathscr{A}(\mathrm{w}, n) = \sum_{|\mathbf{i}| \leq \mathrm{w}+n} \left(\Delta^{i_1} \otimes \cdots \otimes \Delta^{i_n}\right). \tag{20}$$

Equivalently, formula Eq. 20 can be written as[25]

$$\mathscr{A}(\mathrm{w}, n) = \sum_{\mathrm{w}+1 \leq |\mathbf{i}| \leq \mathrm{w}+n} (-1)^{\mathrm{w}+n-|\mathbf{i}|} \binom{n-1}{\mathrm{w}+n-|\mathbf{i}|} \cdot \left(\mathscr{U}^{i_1} \otimes \cdots \otimes \mathscr{U}^{i_n}\right). \tag{21}$$

Given an index set of levels, growth rules must be defined for the one-dimensional quadrature orders. In order to take advantage of nesting and provide similar growth behavior for fully nested and weakly nested integration rules, the following nonlinear growth rules are currently employed:

$$\mathrm{Clenshaw-Curtis}: \quad m = \begin{cases} 1 & w = 0 \\ 2^w + 1 & w \geq 1 \end{cases} \tag{22}$$

$$\mathrm{Gaussian}: \quad m = 2^{w+1} - 1 \tag{23}$$

Examples of isotropic sparse grids, constructed from the fully nested Clenshaw-Curtis abscissas and the weakly-nested Gaussian abscissas are shown in Figure 2, where $\Omega = [-1, 1]^2$. There, we consider a two-dimensional parameter space and a maximum level $\mathrm{w} = 5$ (sparse grid $\mathscr{A}(5, 2)$). To see the reduction in function evaluations with respect to full tensor product grids, we also include a plot of the corresponding Clenshaw-Curtis isotropic full tensor grid having the same maximum number of points in each direction, namely $2^{\mathrm{w}} + 1 = 33$. Whereas an isotropic tensor-product quadrature scales as m^n, an isotropic sparse grid scales as $m^{\log\, n}$, significantly mitigating the curse of dimensionality.

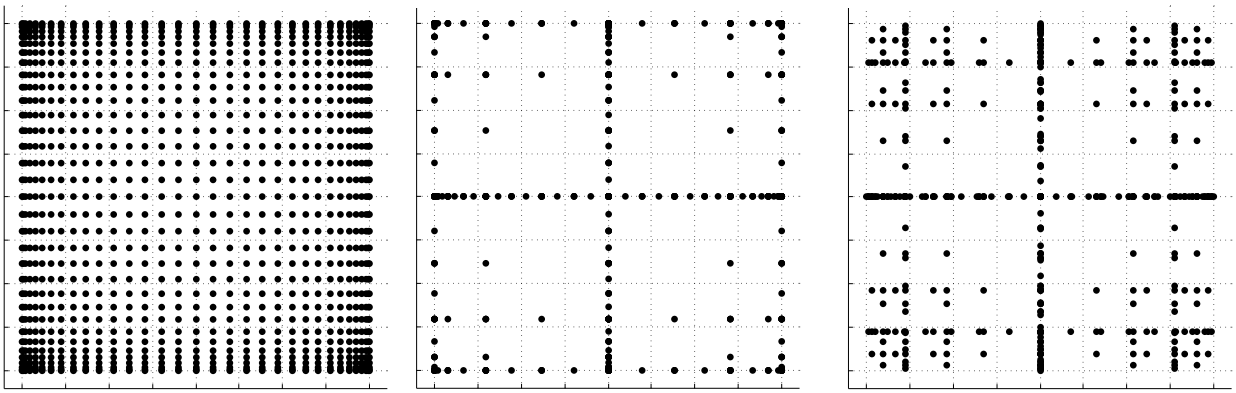

Figure 2. For a two-dimensional parameter space ($n = 2$) and maximum level $\mathrm{w} = 5$, we plot the full tensor product grid using the Clenshaw-Curtis abscissas (left) and isotropic Smolyak sparse grids $\mathscr{A}(5, 2)$, utilizing the Clenshaw-Curtis abscissas (middle) and the Gaussian abscissas (right).

Figure 3 displays the monomial coverage for an isotropic sparse grid with level $w = 4$ employing Gaussian integration rules in two dimensions. Figure 3(a) shows the case of nonlinear growth rules as given in Eq. 23 and Figure 3(b) shows an alternative linear growth rule of $m = 2w + 1$. Given this type of coverage, the traditional approach of exploying a total-order chaos expansion (maximal resolvable total-order integrand

[c]Other common formulations use a dimension-dependent level q where $q \geq n$. We use $w = q - n$, where $w \geq 0$ for all n.

depicted with red horizontal line) can be seen to be well synchronized for the case of linear growth rules and to be somewhat conservative for nonlinear growth rules. Again, the integrand monomial coverage must resolve $2p$, such that $p = 9$ would be selected in the nonlinear growth rule case and $p = 7$ would be selected in the linear growth rule case.

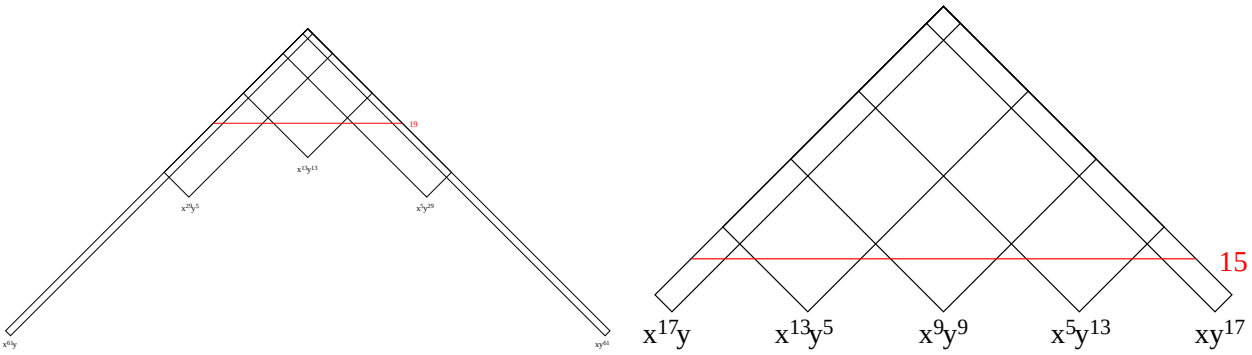

(a) Nonlinear growth rule.

(b) Linear growth rule.

Figure 3. Pascal's triangle depiction of integrand monomial coverage for two dimensions and Gaussian sparse grid level = 4. Red line depicts maximal total-order integrand coverage.

B. Linear regression

The linear regression approach (also known as point collocation or stochastic response surfaces[26, 27]) uses a single linear least squares solution of the form:

$$\boldsymbol{\Psi\alpha} = \boldsymbol{R} \tag{24}$$

to solve for the complete set of PCE coefficients $\boldsymbol{\alpha}$ that best match a set of response values $\boldsymbol{R}$. The set of response values is typically obtained by performing a design of computer experiments within the density function of $\boldsymbol{\xi}$, where each row of the matrix $\boldsymbol{\Psi}$ contains the N_t multivariate polynomial terms Ψ_j evaluated at a particular $\boldsymbol{\xi}$ sample. An over-sampling is generally advisable (Ref. 27 recommends $2N_t$ samples), resulting in a least squares solution for the over-determined system. In the case of $2N_t$ oversampling, the simulation requirements for this approach scale as $\frac{2(n+p)!}{n!p!}$, which can be significantly more affordable than isotropic tensor-product quadrature (e.g., $(p+1)^n$) for larger problems. As for sampling-based coefficient estimation, this approach is only valid for PCE and does not provide any particular monomial coverage guarantee; thus it is common to combine this coefficient estimation approach with a total-order chaos expansion.

A closely related technique is known as the "probabilistic collocation" approach. Rather than employing random over-sampling, this technique uses a selected subset of N_t Gaussian quadrature points (those with highest tensor-product weighting), which provides more optimal collocation locations and preserves interpolation properties.

Finally, additional regression equations can be obtained through the use of derivative information (gradients and Hessians) from each collocation point, which aids greatly in scaling with respect to the number of random variables.

V. Computational Results

Generalized polynomial chaos and stochastic collocation have been implemented in DAKOTA,[28] an open-source software framework for design and performance analysis of computational models on high performance computers. This section compares PCE and SC performance results for several algebraic benchmark test problems. These results build upon PCE results for UQ presented in Ref. 5. In addition, PCE-based and SC-based optimization under uncertainty computational experiments and results are presented in Ref. 29.

A. Lognormal ratio

This test problem has a limit state function (i.e., a critical response metric which defines the boundary between safe and failed regions of the random variable parameter space) defined by the ratio of two correlated, identically-distributed random variables.

$$g(\mathbf{x}) = \frac{x_1}{x_2} \tag{25}$$

The distributions for both x_1 and x_2 are Lognormal(1, 0.5) with a correlation coefficient between the two variables of 0.3. A nonlinear variable transformation is applied and Hermite orthogonal polynomials are employed in the transformed space.

1. Uncertainty quantification with PCE

For the UQ analysis, 24 response levels (.4, .5, .55, .6, .65, .7, .75, .8, .85, .9, 1, 1.05, 1.15, 1.2, 1.25, 1.3, 1.35, 1.4, 1.5, 1.55, 1.6, 1.65, 1.7, and 1.75) are mapped into the corresponding cumulative probability levels. For this problem, an analytic solution is available and is used for comparison to CDFs generated from sampling on the chaos expansions using 10^4, 10^5, or 10^6 samples.

In Figure 4, CDF residuals are plotted for each of the four PCE coefficient estimation approaches on a log-log graph as a function of increasing simulation evaluations. In all cases, an isotropic total-order expansion is used. For the quadrature approach, the expansion order p is varied from 0 to 10, with the quadrature order set at $p + 1$. For the Smolyak sparse grid approach, the level w is varied from 0 to 4, with the expansion order p set based on the empirically-derived heuristic $2p \leq m$ where m is defined from Eq. 23. For the point collocation approach, the expansion order is varied from 0 to 10 with the over-sampling ratio set at 2. And for the sampling approach, the expansion order is fixed at 10 and the expansion samples are varied between 1 and 10^5 by orders of 10. It is evident that the convergence rates for quadrature, sparse grid, and point collocation are super-algebraic/exponential in nature with respect to simulation evaluations, whereas the convergence rate for sampling is algebraic with the expected slope of $-\frac{1}{2}$ (sample estimates converge as the square root of the number of samples). Increasing the number of samples used to numerically evaluate the expansion CDFs (10^4, 10^5, or 10^6 samples) demonstrates that the flat regions in the former three plots are artifacts of the resolution of the sample set, such that these convergence trajectories could be extended further with additional CDF sampling.

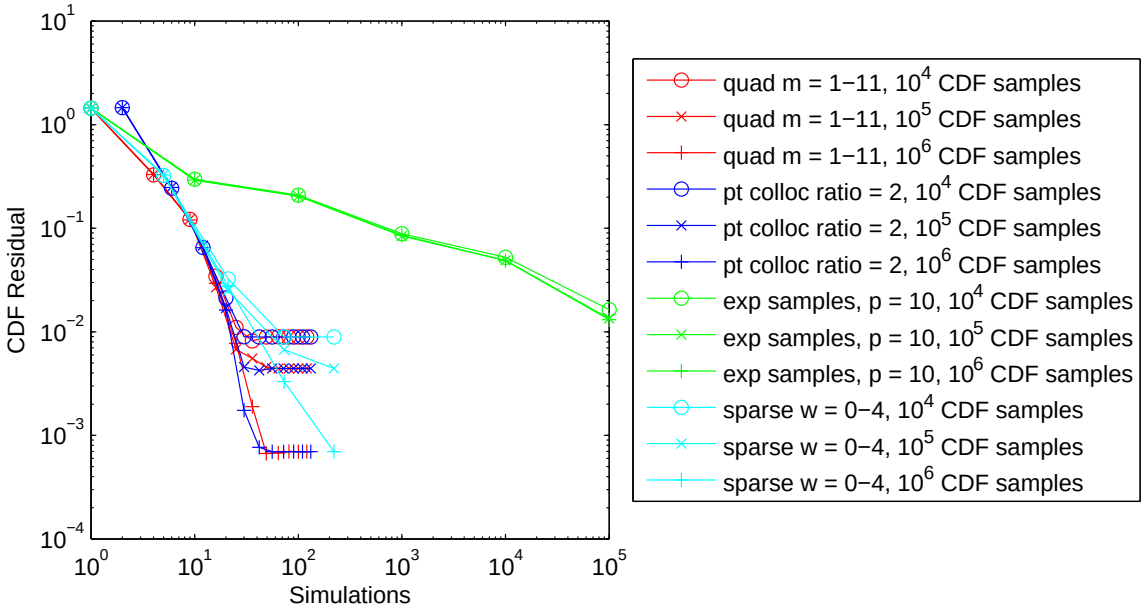

Figure 4. Convergence of traditional PCE with each of the coefficient estimation approaches for the lognormal ratio test problem. CDF residual is shown versus increasing simulation evaluations on a log-log scale.

In Figure 5, the effects of expansion tailoring are demonstrated through use of tensor-product chaos expansions that are synchronized with tensor-product quadrature and use of total-order expansions that

are synchronized with Smolyak sparse grids. The synchronization process in the tensor-product case is straightforward ($p_i = m_i - 1$), whereas the synchronization process in the sparse grid case involves calculation of the maximal total-order expansion that can be resolved within the set of monomials that are integrable by a particular sparse grid, using the process depicted graphically[d] in Figure 3. It is evident that significant accuracy benefits are gained through the use of the tensor-product (tailored) expansions in place of total-order (traditional) expansions when using tensor-product quadrature. For sparse grids, the heuristic rule of thumb (traditional) is shown to be relatively accurate for low dimensions and low levels and only slight gains are realized with the tailored approach for higher levels.

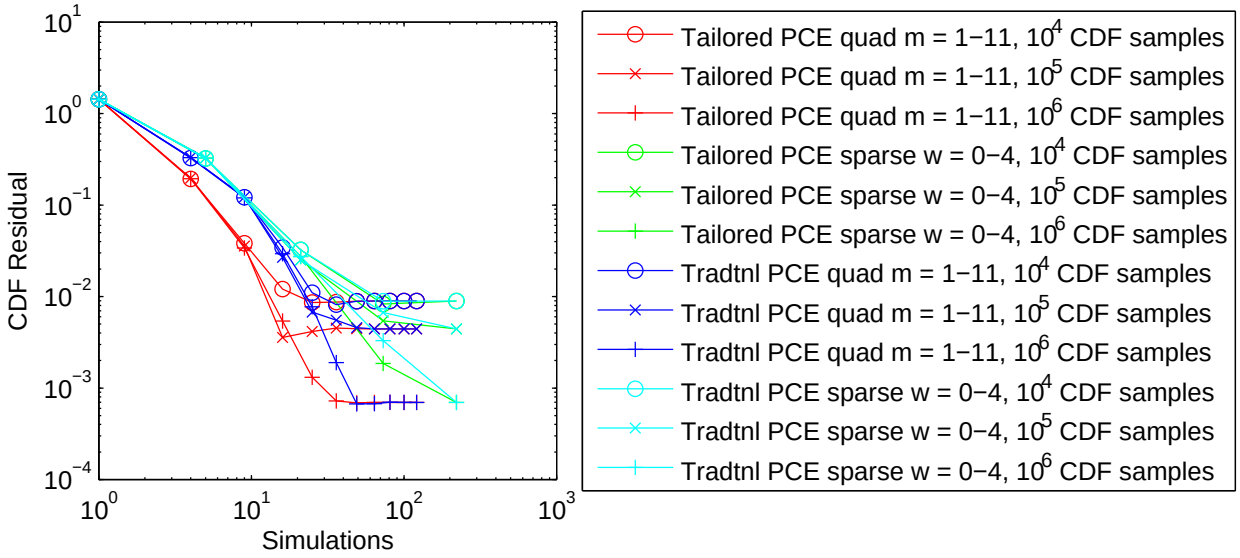

Figure 5. Effect of expansion tailoring on PCE convergence for lognormal ratio test problem.

2. Uncertainty quantification with SC

In Figure 6, convergence results for traditional PCE and SC using quadrature and sparse grids are compared. It is evident that SC outperforms traditional PCE in all cases for this problem.

Finally, Figure 7 compares tensor-product quadrature for traditional PCE (total-order expansion), tailored PCE (tensor-product expansion), and SC and Smolyak sparse grids with nonlinear growth rules for traditional PCE (heuristic total-order), tailored PCE (synchronized total-order), and SC. To reduce clutter, only the most resolved cases (10^6 CDF samples) are shown. It is evident for tensor-product quadrature that tailored PCE not only closes the performance gap between traditional PCE and SC, it completely eliminates it. In fact, a recent analysis[30] demonstrates that synchronized tensor-product PCE and SC can be proven identical for the tensor-product quadrature case. For Smolyak sparse grids, it is evident that tailored PCE is an improvement, but it still falls short of SC performance. It is anticipated that this gap will close further with the use of linear growth rules that reduce computational effort spent resolving polynomials that do appear in the total-order expansion (i.e., polynomials beyond red line in Figure 3(b) versus those in Figure 3(a)).

B. Rosenbrock

The two-dimensional Rosenbrock function is a popular test problem for gradient-based optimization algorithms due to its difficulty for first-order methods. It turns out that this is also a challenging problem for certain UQ methods (especially local reliability methods), since a particular response level contour involves a highly nonlinear curve that may encircle the mean point (leading to multiple most probable points of

[d] A software implementation for the general multidimensional case must track polynomial coverage for both the resolvable integrand and the candidate total-order expansion, which can be done efficiently by storing only the set of Pareto/nondominated monomials for each portion.

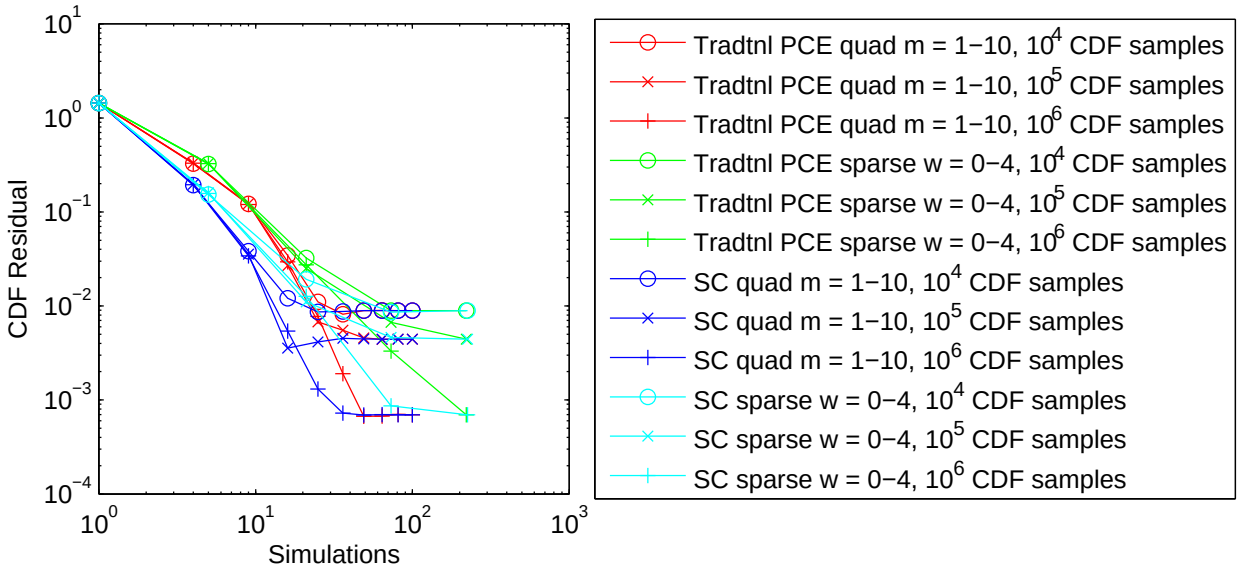

Figure 6. Comparison of SC with traditional PCE for lognormal ratio test problem. CDF residual is shown versus increasing simulation evaluations on a log-log scale.

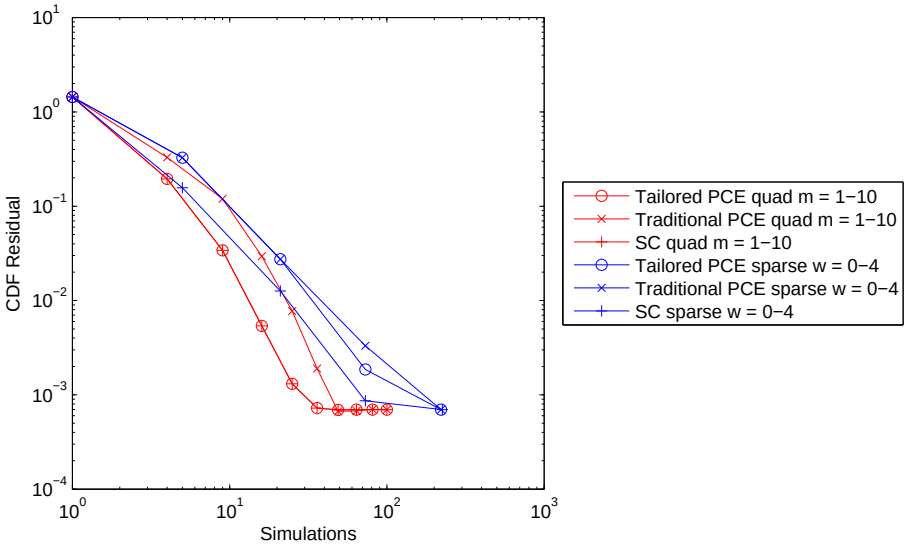

Figure 7. Closing of PCE/SC performance gap using tailored PCE for lognormal ratio test problem. CDF residual evaluated with 10^6 samples.

failure). The function is a fourth order polynomial of the form:

$$f(x_1, x_2) = 100(x_2 - x_1^2)^2 + (1 - x_1)^2 \tag{26}$$

A three-dimensional plot of this function is shown in Figure 8(a), where both x_1 and x_2 range in value from -2 to 2. Figure 8(b) shows a contour plot for Rosenbrock's function where the encircling of a mean value at (0,0) is evident.

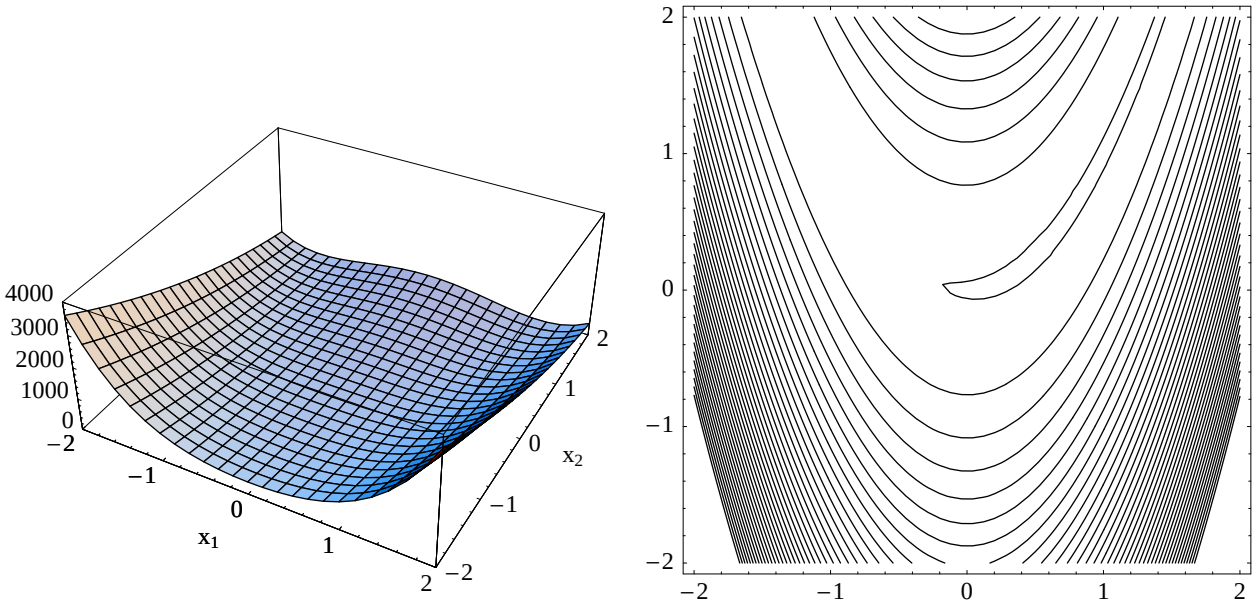

(a) 3-D plot.

(b) Contours.

Figure 8. Rosenbrock's function.

Variables x_1 and x_2 are modeled as independent random variables using normal, uniform, exponential, beta, and gamma probability distributions. A linear variable transformation is used to account for scaling and Askey orthogonal polynomials are employed in the transformed space.

1. Uncertainty quantification with PCE

For the UQ analysis, six response levels (.1, 1., 50., 100., 500., and 1000.) are mapped into the corresponding cumulative probability levels. Since analytic CDF solutions are not available for this problem, accuracy comparisons involve comparisons of statistics generated by sampling on the PCE approximation with statistics generated by sampling on the original response metric, where the sampling sets are of the same size and generated with the same random seed.

In Ref. 5, the expansion order is fixed at four and the exact coefficients are obtained for a quadrature order of five or greater, as expected for integrals (Eq. 15) involving a product of a fourth order function and fourth order expansion terms (refer to Section IV.A.2). Furthermore, with anisotropic quadrature and tensor-product expansions, the function can be integrated exactly with fifth order quadrature in x_1 and third order quadrature in x_2, further reducing the expense from 25 simulations (isotropic) to only 15 simulations (anisotropic).

In Figure 9, the expansion order is again fixed at four, and we vary the distribution type and polynomial basis, including two standard normal variables using a Hermite basis, two uniform variables on $[-2, 2]$ using a Legendre basis, two exponential variables with $\beta = 2$ using a Laguerre basis, two beta variables with $\alpha = 1$ and $\beta = 0.5$ using a Jacobi basis, two gamma variables with $\alpha = 1.5$ and $\beta = 2$ using a generalized Laguerre basis, and five variables (normal, uniform, exponential, beta, and gamma with the same distribution parameters) using a mixed basis. For the mixed expansion over five variables, the standard two-dimensional Rosenbrock is generalized to n-dimensions as defined in Ref. 31. In each case, fifth-order tensor product quadrature is used (25 evaluations each for Hermite, Legendre, Laguerre, Jacobi, and generalized Laguerre

cases, and 3125 evaluations for the mixed case). For the sparse grids over two variables, the Gaussian cases require level = 3 for exact results, at a cost of 73 evaluations for weakly nested (Gauss-Hermite) and 95 evaluations for non-nested (Gauss-Laguerre, Gauss-Jacobi, and generalized Gauss-Laguerre), and the fully-nested Clenshaw-Curtis case requires level = 5 at a cost of 145 evaluations. The five variable mixed Gaussian case requires level = 4 at a cost of 3579 evaluations. In all cases, a fourth-order expansion with sufficient integration is exact as expected, which provides verification of the Askey basis implementation.

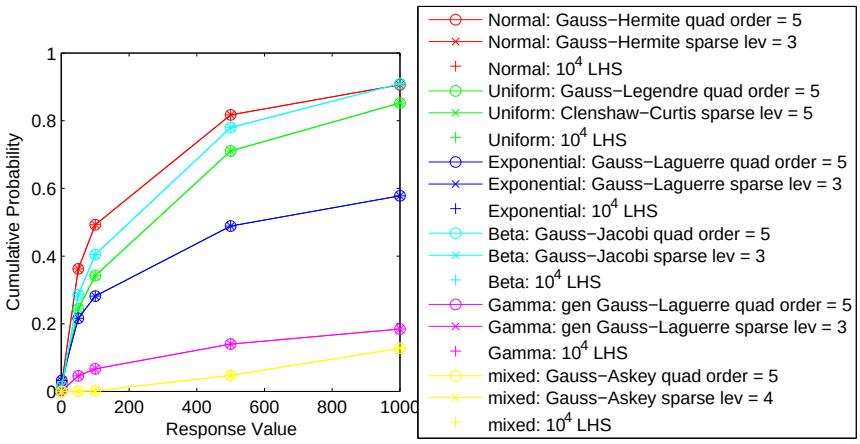

Figure 9. Varying distribution type, PCE basis, and integration approach for Rosenbrock test problem with fixed expansion order = 4.

2. *Uncertainty quantification with SC*

In Figure 10, we reperform the verification tests for SC and the expansion is again exact for sufficient quadrature and sparse grid integration levels. Whereas the integration requirements are the same for PCE

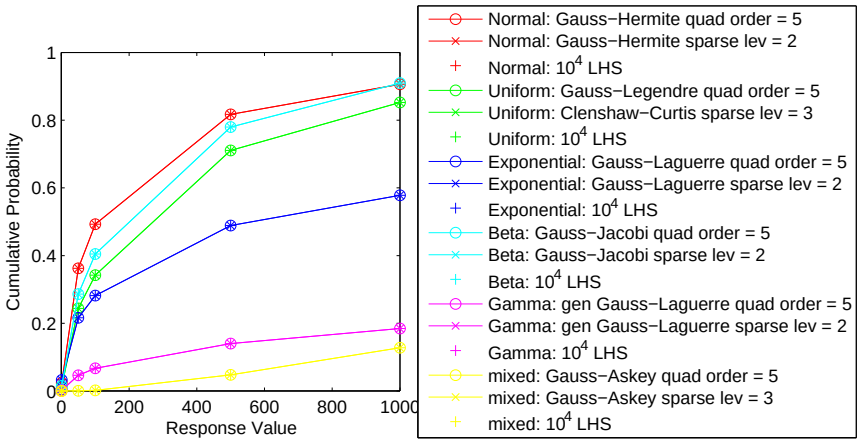

Figure 10. Varying distribution type and collocation point set for SC on the Rosenbrock test problem.

and SC using tensor-product quadrature, an important difference is observed here for sparse grid integration. Whereas PCE requires sparse grid level = 3 for two-dimensional Gaussian rules, sparse grid level = 4 for five-dimensional Gaussian rules, and sparse grid level = 5 for two-dimensional Clenshaw-Curtis to obtain exact results, SC obtains exact results with at least one lower level (level = 2 for two-dimensional Gaussian rules and level = 3 for both two-dimensional Clenshaw-Curtis and five-dimensional Gaussian). In terms of function evaluations, this corresponds to a reduction from 73 to 21 evaluations (two-dimensional Gauss-Hermite, weakly nested), 95 to 29 evaluations (two-dimensional Gauss-Laguerre, Gauss-Jacobi, and generalized Gauss-Laguerre, non-nested), 145 to 29 evaluations (two-dimensional Clenshaw-Curtis, fully nested), and 3579 to 700 evaluations (five-dimensional mixed Gaussian, weakly and non-nested).

C. Short column

This test problem involves the plastic analysis of a short column with rectangular cross section (width $b = 5$ and depth $h = 15$) having uncertain material properties (yield stress Y) and subject to uncertain loads (bending moment M and axial force P).[32] The limit state function is defined as:

$$g(\mathbf{x}) = 1 - \frac{4M}{bh^2Y} - \frac{P^2}{b^2h^2Y^2} \tag{27}$$

The distributions for P, M, and Y are Normal(500, 100), Normal(2000, 400), and Lognormal(5, 0.5), respectively, with a correlation coefficient of 0.5 between P and M (uncorrelated otherwise). A nonlinear variable transformation is applied and Hermite orthogonal polynomials are employed in the transformed space.

1. *Uncertainty quantification with PCE and SC*

Figure 11 shows convergence of mean and standard deviation of the limit state function for increasing quadrature orders and sparse grid levels using tailored PCE, traditional PCE, and SC. Since an analytic solution is not available, residuals are measured relative to an "overkill" solution. The quality of this overkill solution and the effect of compounded roundoff errors can be seen to hinder the convergence trajectories at residual values below 10^{10} (short of double precision machine epsilon). In Figure 11(a), the only discernable

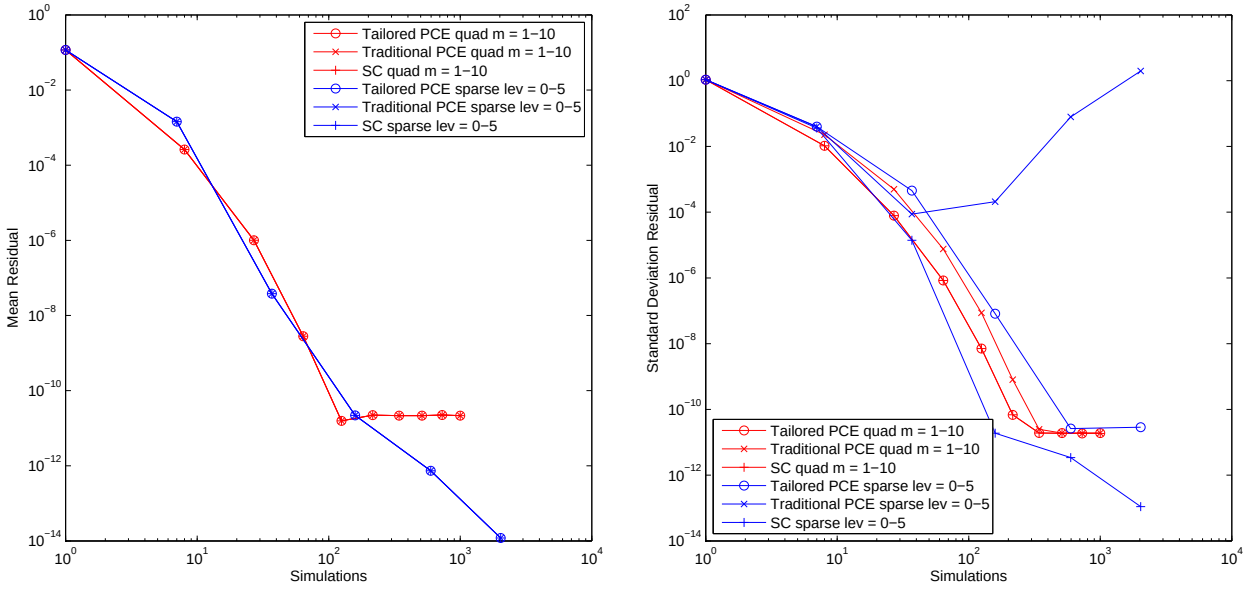

(a) Mean residual.

(b) Standard deviation residual.

Figure 11. Convergence of mean and standard deviation for the short column test problem.

difference appears between the set of quadrature results and the set of sparse grid results, with similar performance between the two sets. In Figure 11(b), however, significant differences are evident. First, for tensor-product quadrature, tensor-product PCE (tailored) is again shown to completely eliminate the performance gap between total-order PCE (traditional) and SC. For sparse grids, the heuristic total-order PCE approach (traditional) is shown to be nonconservative for this problem in its estimation of the order of expansion to employ. Through inclusion of monomials that exceed the order of what can be resolved, the expansion standard deviation fails to converge. The synchronized total-order PCE approach (tailored) is shown to be more rigorous, although its performance falls well short of that of SC with sparse grids. Without this rigorous estimation, however, one would be left with the undesirable alternative of trial and error in synchronizing the sparse grid with a PCE expansion order. Whereas tensor-product quadrature outperformed sparse grids for the two-dimensional problem in Figure 7 (such that the equivalent tailored PCE and SC tensor-product quadrature approaches performed the best), this trend has started to reverse with the increase to three dimensions and SC with sparse grids stands alone as the most efficient technique.

D. Cantilever beam

The next test problem involves the simple uniform cantilever beam[33,34] shown in Figure 12. Random

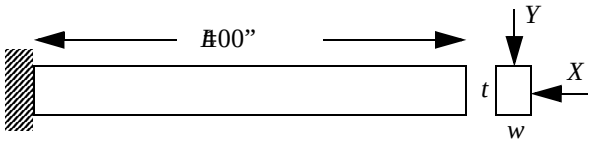

Figure 12. Cantilever beam test problem.

variables in the problem include the yield stress R and Youngs modulus E of the beam material and the horizontal and vertical loads, X and Y, which are modeled with normal distributions using N(40000, 2000), N(2.9E7, 1.45E6), N(500, 100), and N(1000, 100), respectively. Problem constants include $L = 100$ in. and $D_0 = 2.2535$ in. The beam response metrics have the following analytic form:

$$\text{stress} = \frac{600}{wt^2}Y + \frac{600}{w^2t}X \leq R \tag{28}$$

$$\text{displacement} = \frac{4L^3}{Ewt}\sqrt{(\frac{Y}{t^2})^2 + (\frac{X}{w^2})^2} \leq D_0 \tag{29}$$

These stress and displacement response functions are scaled using $\frac{\text{stress}}{R} - 1$ and $\frac{\text{displacement}}{D_0} - 1$, such that negative values indicate safe regions of the parameter space. A linear variable transformation is used to account for scaling of the normal PDFs and Hermite orthogonal polynomials are employed in the transformed space.

1. *Uncertainty quantification with PCE and SC*

Figure 13 shows convergence of the mean residuals and Figure 14 shows convergence of the standard deviation residuals for scaled stress and displacement for increasing quadrature orders and sparse grid levels using tailored PCE, traditional PCE, and SC. An analytic solution is again unavailable, so residuals are measured relative to an "overkill" solution such that convergence again slows at residual values below 10^{-10}. In

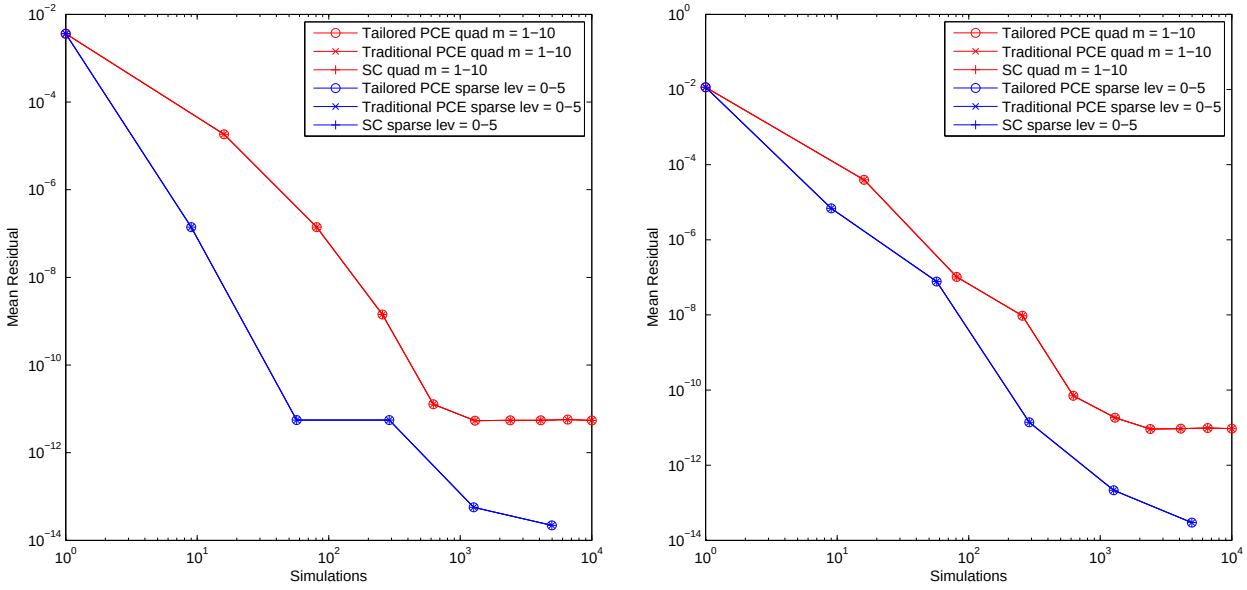

(a) Scaled stress.

(b) Scaled displacement.

Figure 13. Convergence of mean for PCE and SC in the cantilever beam test problem.

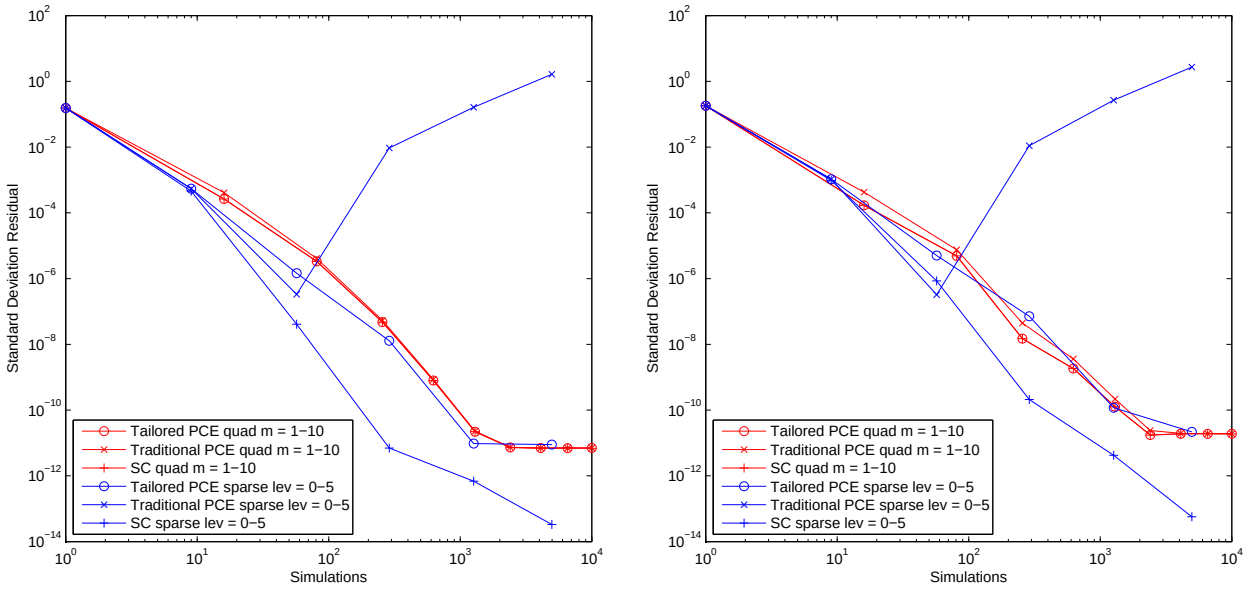

(a) Scaled stress.

(b) Scaled displacement.

Figure 14. Convergence of standard deviation for PCE and SC in the cantilever beam test problem.

Figure 13, the only discernable difference appears between the set of quadrature results and the set of sparse grid results, with sparse grids outperforming tensor-product quadrature for this four-dimensional problem. In Figure 14, additional differences are again evident. For tensor-product quadrature, the performance gap between total-order PCE (traditional) and SC is relatively small, but tensor-product PCE (tailored) is again shown to completely eliminate it. For sparse grids, the heuristic total-order PCE approach (traditional) is again shown to be nonconservative in its estimation of the order of expansion to employ, and the synchronized total-order PCE approach (tailored) is shown to be more rigorous, although it again falls short of the performance of SC. As for the previous three-dimensional problem (Figure 11(b)), SC with sparse grids stands alone as the most efficient technique.

VI. Conclusions

This paper has investigated the relative performance of non-intrusive generalized polynomial chaos and stochastic collocation methods applied to several algebraic benchmark problems with known solutions. The primary distinction between these methods is that PCE must estimate coefficients for a known basis of orthogonal polynomials (using sampling, linear regression, quadrature, or sparse grids) whereas SC must form an interpolant for known coefficients (using quadrature or sparse grids).

Performance between these methods is shown to be very similar and both demonstrate impressive efficiency relative to Monte Carlo sampling methods and impressive accuracy relative to reliability methods. When a difference is observed between traditional PCE and SC, SC has been the consistent winner, typically manifesting in the reduction of the required integration by one order or level. This difference can be largely attributed to expansion/integration synchronization issues with PCE, motivating the approaches for tailoring of chaos expansions that are explored in this paper.

For the case of tensor-product quadrature, tailored tensor-product PCE is shown to perform identically to SC such that the performance gap is completely eliminated. Both methods consistently outperform traditional PCE. However, tensor-product quadrature approaches only outperform sparse grid approaches for the lowest dimensional problems.

For problems with greater than two dimensions, sparse grid approaches are shown to outperform tensor-product quadrature approaches. For sparse grids, selection of a synchronized PCE formulation is nontrivial and the tailored total-order PCE approach, which computes the maximal total-order expansion that can be resolved by a particular sparse grid, is shown to be more rigorous and reliable than heuristics and eliminates

inefficiency due to trial and error. A significant performance gap relative to SC with sparse grids still remains for the case of nonlinear sparse grid growth rules, but replacement of these rules with linear ones (at least for Gaussian quadratures that are not fully nested) will reduce the set of resolvable polynomials that do not appear in the total-order expansion. This is expected to close the performance gap to some degree. However, it is not expected that any nonintrusive PCE approach will outperform SC when using the same set of collocation points. Rather, usage of PCE remains motivated by other practical considerations, in particular its greater flexibility in collocation point selection (i.e., cubature grids as well as unstructured/random point sets that can support greater simulation fault tolerance).

Future work will investigate these linear sparse grid growth rules as well as sparse grids that support anisotropy in level and numerically-generated polynomials that preserve exponential convergence rates for arbitrary input PDFs.

Acknowledgments

The authors thank Paul Constantine and Gianluca Iaccarino of Stanford University for sharing their analysis on the equivalence of tensor-product PCE and SC, which largely motivated the exploration of PCE tailoring in this work. The authors also thank Clayton Webster for his development of concepts and analysis for anisotropic sparse grids. Finally, the authors thank the DOE Accelerated Strategic Computing (ASC) program for support of this collaborative work between Sandia National Laboratories and Virginia Tech.

References

[1]Xiu, D. and Karniadakis, G. M., "The Wiener-Askey Polynomial Chaos for Stochastic Differential Equations," *SIAM J. Sci. Comput.*, Vol. 24, No. 2, 2002, pp. 619–644.

[2]Askey, R. and Wilson, J., "Some Basic Hypergeometric Polynomials that Generalize Jacobi Polynomials," *Mem. Amer. Math. Soc. 319*, AMS, Providence, RI, 1985.

[3]Wiener, N., "The Homogoeneous Chaos," *Amer. J. Math.*, Vol. 60, 1938, pp. 897–936.

[4]Abramowitz, M. and Stegun, I. A., *Handbook of Mathematical Functions with Formulas, Graphs, and Mathematical Tables*, Dover, New York, 1965.

[5]Eldred, M. S., Webster, C. G., and Constantine, P., "Evaluation of Non-Intrusive Approaches for Wiener-Askey Generalized Polynomial Chaos," *Proceedings of the 10th AIAA Nondeterministic Approaches Conference*, No. AIAA-2008-1892, Schaumburg, IL, April 7–10 2008.

[6]Der Kiureghian, A. and Liu, P. L., "Structural Reliability Under Incomplete Probability Information," *J. Eng. Mech., ASCE*, Vol. 112, No. 1, 1986, pp. 85–104.

[7]Golub, G. H. and Welsch, J. H., "Caclulation of Gauss Quadrature Rules," *Mathematics of Computation*, Vol. 23, No. 106, 1969, pp. 221–230.

[8]Witteveen, J. A. S. and Bijl, H., "Modeling Arbitrary Uncertainties Using Gram-Schmidt Polynomial Chaos," *Proceedings of the 44th AIAA Aerospace Sciences Meeting and Exhibit*, No. AIAA-2006-0896, Reno, NV, January 9–12 2006.

[9]Eldred, M. S., "Recent Advances in Non-Intrusive Polynomial Chaos and Stochastic Collocation Methods for Uncertainty Analysis and Design," *to appear in Proceedings of the 11th AIAA Nondeterministic Approaches Conference*, No. AIAA-2009-2274, Palm Springs, CA, May 4–7 2009.

[10]Ghanem, R. G., private communication.

[11]Eldred, M. S., Agarwal, H., Perez, V. M., Wojtkiewicz, Jr., S. F., and Renaud, J. E., "Investigation of Reliability Method Formulations in DAKOTA/UQ," *Structure & Infrastructure Engineering: Maintenance, Management, Life-Cycle Design & Performance*, Vol. 3, No. 3, 2007, pp. 199–213.

[12]Eldred, M. S. and Bichon, B. J., "Second-Order Reliability Formulations in DAKOTA/UQ," *Proceedings of the 47th AIAA/ASME/ASCE/AHS/ASC Structures, Structural Dynamics and Materials Conference*, No. AIAA-2006-1828, Newport, RI, May 1–4 2006.

[13]Rosenblatt, M., "Remarks on a Multivariate Transformation," *Ann. Math. Stat.*, Vol. 23, No. 3, 1952, pp. 470–472.

[14]Box, G. E. P. and Cox, D. R., "An Analysis of Transformations," *J. Royal Stat. Soc.*, Vol. 26, 1964, pp. 211–252.

[15]Rackwitz, R. and Fiessler, B., "Structural Reliability under Combined Random Load Sequences," *Comput. Struct.*, Vol. 9, 1978, pp. 489–494.

[16]Chen, X. and Lind, N. C., "Fast Probability Integration by Three-Parameter Normal Tail Approximation," *Struct. Saf.*, Vol. 1, 1983, pp. 269–276.

[17]Wu, Y.-T. and Wirsching, P. H., "A New Algorithm for Structural Reliability Estimation," *J. Eng. Mech., ASCE*, Vol. 113, 1987, pp. 1319–1336.

[18]Nobile, F., Tempone, R., and Webster, C. G., "A Sparse Grid Stochastic Collocation Method for Partial Differential Equations with Random Input Data," *SIAM J. on Num. Anal.*, 2008, To appear.

[19]Nobile, F., Tempone, R., and Webster, C. G., "An Anisotropic Sparse Grid Stochastic Collocation Method for Partial Differential Equations with Random Input Data," *SIAM J. on Num. Anal.*, 2008, To appear.

[20]Gerstner, T. and Griebel, M., "Numerical integration using sparse grids," *Numer. Algorithms*, Vol. 18, No. 3-4, 1998, pp. 209–232.

[21]Smolyak, S., "Quadrature and interpolation formulas for tensor products of certain classes of functions," *Dokl. Akad. Nauk SSSR*, Vol. 4, 1963, pp. 240–243.

[22]Barthelmann, V., Novak, E., and Ritter, K., "High dimensional polynomial interpolation on sparse grids," *Adv. Comput. Math.*, Vol. 12, No. 4, 2000, pp. 273–288, Multivariate polynomial interpolation.

[23]Frauenfelder, P., Schwab, C., and Todor, R. A., "Finite elements for elliptic problems with stochastic coefficients," *Comput. Methods Appl. Mech. Engrg.*, Vol. 194, No. 2-5, 2005, pp. 205–228.

[24]Xiu, D. and Hesthaven, J., "High-order collocation methods for differential equations with random inputs," *SIAM J. Sci. Comput.*, Vol. 27, No. 3, 2005, pp. 1118–1139 (electronic).

[25]Wasilkowski, G. W. and Woźniakowski, H., "Explicit Cost Bounds of Algorithms for Multivariate Tensor Product Problems," *Journal of Complexity*, Vol. 11, 1995, pp. 1–56.

[26]Walters, R. W., "Towards Stochastic Fluid Mechanics via Polynomial Chaos," *Proceedings of the 41st AIAA Aerospace Sciences Meeting and Exhibit*, No. AIAA-2003-0413, Reno, NV, January 6–9, 2003.

[27]Hosder, S., Walters, R. W., and Balch, M., "Efficient Sampling for Non-Intrusive Polynomial Chaos Applications with Multiple Uncertain Input Variables," *Proceedings of the 48th AIAA/ASME/ASCE/AHS/ASC Structures, Structural Dynamics, and Materials Conference*, No. AIAA-2007-1939, Honolulu, HI, April 23–26, 2007.

[28]Eldred, M. S., Adams, B. M., Haskell, K., Bohnhoff, W. J., Eddy, J. P., Gay, D. M., Hart, W. E., Hough, P. D., Kolda, T. G., Swiler, L. P., and Watson, J.-P., "DAKOTA, A Multilevel Parallel Object-Oriented Framework for Design Optimization, Parameter Estimation, Uncertainty Quantification, and Sensitivity Analysis: Version 4.2 Users Manual," Tech. Rep. SAND2006-6337, Sandia National Laboratories, Albuquerque, NM, 2008.

[29]Eldred, M. S., Webster, C. G., and Constantine, P., "Design Under Uncertainty Employing Stochastic Expansion Methods," *Proceedings of the 12th AIAA/ISSMO Multidisciplinary Analysis and Optimization Conference*, No. AIAA-2008-6001, Victoria, British Columbia, September 10–12, 2008.

[30]Constantine, P. and Iaccarino, G., "Comparing spectral Galerkin and spectral collocation methods for parameterized matrix equations." Tech. Rep. UQ-08-02, Stanford University, Stanford, CA, 2008.

[31]Schittkowski, K., *More Test Examples for Nonlinear Programming, Lecture Notes in Economics and Mathematical Systems, Vol. 282*, Springer-Verlag, Berlin, 1987.

[32]Kuschel, N. and Rackwitz, R., "Two Basic Problems in Reliability-Based Structural Optimization," *Math. Method Oper. Res.*, Vol. 46, 1997, pp. 309–333.

[33]Sues, R., Aminpour, M., and Shin, Y., "Reliability-Based Multidisciplinary Optimization for Aerospace Systems," *Proceedings of the 42rd AIAA/ASME/ASCE/AHS/ASC Structures, Structural Dynamics, and Materials Conference*, No. AIAA-2001-1521, Seattle, WA, April 16–19, 2001.

[34]Wu, Y.-T., Shin, Y., Sues, R., and Cesare, M., "Safety-Factor Based Approach for Probability-Based Design Optimization," *Proceedings of the 42rd AIAA/ASME/ASCE/AHS/ASC Structures, Structural Dynamics, and Materials Conference*, No. AIAA-2001-1522, Seattle, WA, April 16–19, 2001.